EgGLUT1 is crucial for the viability of larvae of *Echinococcus granulosus sensus lato* by involving its glucose uptake

Kuerbannisha Amahong[a,b*], Mingzhi Yan[a,b*], Jintian Li[a,b], Ning Yang[a], Hui Liu[a], Xiaojuan Bi[a], Dominique A. Vuitton[c], Renyong Lin[a, d, e**] and Guodong Lü[a,b,d**]

[a]State Key Laboratory of Pathogenesis, Prevention, and Treatment of Central Asian High Incidence Diseases, Clinical Medical Research Institute, The First Affiliated Hospital of Xinjiang Medical University, Urumqi, China

[b]College of Pharmacy, Xinjiang Medical University, Urumqi, China

[c]University Bourgogne Franche-Comté and French National Reference Centre for Echinococcosis, Besançon, France

[d]WHO Collaborating Centre for Prevention and Care Management of Echinococcosis, The First Affiliated Hospital of Xinjiang Medical University, Urumqi, China

[e]Basic Medical College, Xinjiang Medical University, Urumqi, China

*These authors should be considered joint first authors.

** Correspondence to Guodong Lü and Renyong Lin

**Corresponding author: Guodong Lü. The First Affiliated Hospital of Xinjiang Medical University, Room 425, KE JI Building, No. 137 Liyushan Road Urumqi, Xinjiang 830054. E-mail: lgd_xj@qq.com. Renyong Lin. The First Affiliated Hospital of Xinjiang Medical University, Room 425, KE JI Building, No. 137 Liyushan Road Urumqi, Xinjiang 830054. E-mail: renyonglin@xjmu.edu.cn.

ABSTRACT

Cystic echinococcosis (CE) is a zoonotic parasitic disease caused by infection with the larvae of *Echinococcus granulosus sensu lato* (*s.l.*) cluster. It is urgent to identify novel drug targets and develop new drug candidates against CE. Glucose transporter 1 (GLUT1) is mainly responsible for the transmembrane transport of glucose to maintain its constant cellular availability and is a recent research hotspot as a drug target in various diseases. However, presence and role of GLUT1 in *E. granulosus s.l.* (EgGLTU1) was unknown. In this study, we cloned a conserved GLUT1 homology gene (named EgGLUT1-ss) from *E. granulosus sensu stricto* (*s.s.*) and found EgGLUT1-ss was crucial for glucose uptake of the protoscoleces of *E. granulosus s.s.*. WZB117, a GLUT1 inhibitor, inhibited glucose uptake of *E. granulosus s.s.* and the viability of the metacestode *in vitro.* In addition, WZB117 showed potent therapeutic activity in *E. granulosus s.s.*-infected mice: a 10 mg/kg dose of WZB117 significantly reduced the number and weight of parasite cysts as well as the reference drug, albendazole. Our data have defined EgGLUT1 as a key *E. granulosus s.l.* vulnerability target, involved in its glucose uptake from the host; this opens a new avenue to identify drugs with an ideal activity profile for the treatment of CE.

Keywords: cystic echinococcosis; glucose transporter 1; glucose uptake; WZB117

Introduction

Cystic echinococcosis (CE) is a chronic and neglected zoonotic parasitic disease caused by the larvae of the *Echinococcus granulosus sensu lato* (*s.l.*) cluster and listed

as one of 17 neglected tropical diseases by the World Health Organization (WHO) (1). CE is distributed worldwide, mainly in South America, Eastern Europe, the Middle East, Russia, and Western China, and the incidence is up to 5% to 10% in highly endemic areas (2,3). More than 2-3 million cases are estimated worldwide (4). According to the WHO, the costs globally committed for treating CE are more than $3 billion per year (5). China has a high prevalence of human CE, accounting for 40 % of global DALYs lost worldwide (6). Between 2012 and 2016, CE was endemic in 368 counties, with an estimated 166,098 cases of CE in China (7).

The early symptoms of CE are not obvious, and most CE patients are already in advanced stages when they seek medical treatment (2). This treatment mainly includes surgical and anti-parasitic drug treatments, but surgery is not always possible and may be complicated by postoperative recurrence and secondary infection or biliary leakage (8). For some patients who are not suitable for surgical treatment, antiparasitic treatment has become the first choice; in this situation, the germinal layer of the metacestode is the main target of the drug. Anti-parasitic treatment is also used before and after operation to prevent a recurrence, with the possibly spilled protoscoleces (PSCs) as main targets (9). Currently, benzimidazoles, mebendazole and more often albendazole (ABZ), are the only drugs that may be used to treat this infection at its metacestode stage, as recommended by WHO, but such drugs are characterized by poor bioavailability, wide inter-individual variations in blood levels, and occurrence of adverse reactions (10, 11). At present, we are missing anti-CE

drugs that can effectively replace ABZ; in addition, the killing potential of ABZ on PSCs is not optimal, and it is delayed (11). Therefore, the identification of new drug targets and the development of new therapeutic molecules are of great significance for the treatment of CE.

The results of transcriptome and whole-genome sequencing show that after entering the intermediate host, the anabolic ability of *E. granulosus s.l.* is severely degraded, while its ability to absorb nutrients is greatly increased, and complete metabolic pathways such as glycolysis, tricarboxylic acid cycle and pentose phosphate cycles function efficiently (12, 13). This suggests that *E. granulosus s.l.* requires nutrients such as glucose from the intermediate host's environment to meet basic physiological functions such as energy metabolism. If glucose is not transported from the host environment in time or cannot be transported to the parasite, the parasite's death probably occurs, which is suggested by the presence of specific antibodies to *E. granulosus s.l.* in the serum of patients without lesions in endemic areas, and the observation of abortive forms of disease (14). It is considered that interference with glucose metabolism is one of the mechanisms of action of ABZ (15). However, the precise metabolic chain involved in *E. granulosus s.l.* glucose uptake is unknown.

Glucose transporter 1 (GLUT1) is widely distributed across most cell types and responsible for the transmembrane transport of glucose (16). In recent years, GLUT1 has gradually become a research hotspot in the field of metabolic diseases, cancer, and

85 other diseases, and is considered as an important target for drug development (17-19).
86 Recently, Wei *et al.* found that inhibiting the human GLUT1 in the erythrocytes could
87 alleviate their injury caused by *Plasmodium* spp. Infection (20). For some parasites,
88 such as *Trypanosoma* spp. and *Leishmania* spp., hexose transporters have been
89 reported to be involved in the glucose uptake pathway of the parasite (21, 22). In
90 addition, GLUT1 of *E. multilocularis* was shown to have relatively high glucose
91 transport activity and to be a crucial participant in the parasite glucose metabolism
92 (23). WZB117, which binds to the GLUT1 at the exofacial sugar binding site, is a
93 reversible competitive inhibitor of glucose uptake and exchange glucose transport
94 (24), and has now been shown to have therapeutic effects in cancer (25) and
95 *Plasmodium* infection (20). However, we currently do not know whether GLUT1 can
96 be an important drug target in echinococcosis treatment and whether its inhibitor
97 WZB117 has an anti-cystic echinococcosis effect.

98 In our study, we tested whether we could affect *E. granulosus s.l.* glucose uptake
99 by targeting EgGLUT1 at the metacestode stage of *E. granulosus s.l.*. We thus cloned
100 a conserved GLUT1 homology gene from *E. granulosus sensu stricto* (*s.s.*), the
101 species most widely responsible for CE cases worldwide, and inhibited EgGLUT1 by
102 WZB117 to study its possible impact on the survival of the metacestode *in vitro* and
103 in an experimental animal model.

104 ## Results

105 **Cloning, and physiological and biochemical characterization of EgGLUT1-ss**

106 To assess whether GLUT1 gene was present in *E. granulosus s.s*, we
107 successfully cloned a conserved GLUT1 homologous gene from *E. granulosus s.s.*,
108 named EgGLUT1-ss (accession number: MW393831) (Supplementary Figure 1),
109 which consists of 500 amino acids (Figure 1a). Bioinformatics analysis showed that
110 EgGLUT1-ss had one major facilitator superfamily (MFS) domain and 12
111 transmembrane regions, which were a typical feature of the GLUT gene (Figure 1a).
112 This special structure plays an important role in the transmembrane transport of
113 glucose (26). In addition, we also found that EgGLUT1-ss contained two amidation
114 sites, one glycosylation site, one cAMP- and cGMP-dependent protein kinase
115 phosphorylation site, two casein kinase II phosphorylation sites, five myristoylation
116 sites, and five protein kinase C phosphorylation sites (Figure 1a). Whole sequence
117 alignment analysis showed that the highest overall homologies on the amino acid
118 sequence level could be detected between EgGLUT1-ss and the GLUT1 of *E.*
119 *multilocularis* (96.81% identical); and GLUT1 orthologs were found in various other
120 species (with a 32.77% to 72.33% homology) (Figure 1a). Phylogenetic analysis
121 revealed that the EgGLUT1-ss gene was generally closely related to parasite species
122 GLUT genes, especially helminths, and was more distantly related to mammalian
123 species such as human and mouse GLUT genes (Figure 1b).

124 **EgGLUT1-ss Knockdown reduces the viability and glucose uptake of *E.***
125 ***granulosus s.s.* PSCs**

126 To investigate EgGLTU1 function in *E. granulosus s.l.*, we examined the

EgGLUT1-ss expression in PSCs and vesicles of *E. granulosus s.s.*. We found EgGLUT1-ss was expressed in both PSCs and vesicles, and EgGLUT1-ss expression level in PSCs was 3.5 times higher than that of vesicles (Figure 2a).

To determine the functional relevance of EgGLUT1-ss in PSCs, we designed three siRNA sequences (siRNA-386/578/723) targeting EgGLUT1-ss. The siRNA-386/578/723 treatment led to a significant reduction in EgGLUT1-ss-mRNA expression of PSCs (Figure 2b) and decreased PSCs viability considerably (Figure 2c). To examine the influence of EgGLUT1-ss knockdown on the glucose uptake of PSCs, siRNA-386/578/723 were transfected into PSCs, and 2 days after transfection, 2-NBDG uptake by PSCs decreased significantly (Figure 2d).

WZB117 inhibits glucose metabolism and reduces the viability of *E. granulosus s.s.* PSCs *in vitro*

By docking predictions, we found that WZB117 had the potential ability to combine with EgGLUT1-ss. The binding of WZB117 to EgGLUT1-ss involved four hydrogen bonds, with Arg120, Asn29, Asn285 and Gln280. Amino acid residues Phe66, Thr25, Val63, Phe289, Ala286, and Trp410 interacted with the WZB117 molecule through hydrophobic bonds (Figure 3a). After 60 min incubation with WZB117 *in vitro*, the glucose uptake level of PSCs was significantly decreased (Figure 3b). After 48 hours incubation with 25, 50, and 100 μmol/L WZB117 *in vitro*, the glucose content of PSCs was significantly decreased (Figure 3c). In parallel, the ATP content was decreased (Figure 3d) when the PSCs were treated with 50 and 100

μmol/L WZB117.

To investigate the WZB117 inhibition effect on the viability of *E. granulosus s.s.* larval stages *in vitro*, we analyzed the survival rate of PSCs exposed to various WZB117 concentrations. As shown in Figure 3e, compared to the control group, 4 days-WZB117 exposure led to a dose-dependent decrease in the viability of PSCs in cultures. After exposure to 100 μmol/L WZB117 *in vitro* for one day, all the PSCs died. Scanning electronic microscopy (SEM) showed that, compared to the control group, WZB117-treated PSCs exhibited incomplete rostellum structure, absence of hooks, collapsed suckers and various damages to the other structures of the PSCs, as shown in Figure 3f. Transmission electronic microscopy (TEM) showed that there were significant changes in the ultrastructure of WZB117-treated PSCs: the microtriches disappeared, the nuclei were ruptured, associated with disappearance of the nucleoli, and vacuoles appeared in the cytoplasm. (Figure 3g).

WZB117 reduces the viability of *E. granulosus s.s.* vesicles *in vitro*

Cysts are the lesions produced by *E. granulosus s.l.* in the intermediate host and their development is related to the pathogenicity of this helminth (2). Therefore, we further explored the effect of WZB117 on such *in vitro*-cultured vesicles exposed to increasing concentrations of WZB117. The viability of the vesicles was significantly decreased when they were exposed to various concentrations of WZB117 for 4 days; it was decreased by 100% on day 3 when exposed to 100 μmol/L WZB117 (Figure 4a). These data and morphological changes indicate that WZB117 had a significant

169 effect on the reduction of the viability of *in vitro*-developed *E. granulosus s.s.* vesicles.
170 Compared with the control group, the SEM features of the vesicles in the WZB117
171 group changed significantly: the germinal layer was condensed, and the vesicles
172 collapsed. The degree of collapse was positively correlated with the dose of
173 WZB1117 (Figure 4b). TEM images obtained from the WZB117-treated vesicles
174 showed that the structures of germinal layer and laminated layer were damaged, lipid
175 droplet appeared, the microtriches were reduced, nucleoli disappeared, the
176 heterochromatin edges were clustered, and the cortical matrix was fuzzy (Figure 4c).

177 **WZB117 treatment affects glucose/ATP levels and effectively prevents the growth**
178 **and of cysts in *E. granulosus s.s.*-infected mice**

179 We measured the glucose and ATP content of the cysts *in vivo*. There was a
180 marked reduction in glucose and ATP levels in the cyst tissue; the reduction was less
181 marked in the cyst fluid (Figure 5a and b). A significant reduction of glucose and ATP
182 levels in the cyst fluid was observed for the 20 mg/kg dose of WZB117 (Figure 5c and
183 d).

184 After 6 months of WZB117 treatment, the weight of cysts recovered from
185 WZB117-treated mice was significantly lower than that recovered from the control
186 group (Figure 5e). Additionally, the number and diameter of cysts in WZB117-treated
187 mice were lower than those of the control group (Figure 5f and g). Overall, the
188 'therapeutic' effect of 10 mg/kg WZB117 was comparable to that of ABZ (Figure 5h).

189 In the control group (Figure 5i), the cysts had no significant structural

abnormalities when observed with TEM. However, the structure of cysts removed from the treated groups was damaged at different degrees (Figure 5i). Compared with the control group, cysts from WZB117-treated mice had loose germinal layers, the microtriches were shortened and reduced dramatically in length, the tegument was thinned, the structure of the laminated layer was destroyed, and the nuclei were condensed.

For a preliminary assessment of the safety of WZB117 in the treatment of CE in experimental hosts, we measured the usual indices of adverse effects. There were no differences in body weight between treated and control mice. The aspartate transaminase (AST) level was significantly lower in the 5 mg/kg WZB117-treated groups than in the control group (Supplementary Figure 2a) and there were no significant differences in alanine aminotransferase (ALT) and alkaline phosphatase (ALP) levels, the most accurate markers of liver damage (Supplementary Figure 2b and c). The 5 mg/kg WZB117-treated group had lower blood urea levels than the control group (Supplementary Figure 2d) but all observed values remained in the physiological range and creatinine levels were similar in all WZB117-treated groups and in the control group (Supplementary Figure 2e). Blood glucose levels were also not different in WZB117-treated mice and in control mice (Supplementary Figure 3). Overall, WZB117, at the dosages used in our study did not cause significant toxicity in mice.

Discussion

The energy-associated metabolic pathways are essential for the survival of parasites and their adaptation to their successive hosts (27); glucose metabolism is the main energy source (12). Glucose metabolism pathways, especially glycolysis, had been evidenced as a target for anti-echinococcosis drugs (28). However, the upstream pathway of glucose metabolism in *E. granulosus s.l.*, which is involved in glucose uptake from the host, was still elusive. In this study, we identified EgGLUT1-ss as a crucial protein involved in glucose uptake by *E. granulosus s.s.* metacestode and demonstrated that functional EgGLUT1-ss was essential for energy-sourcing and survival in the intermediate host of the parasite. We also characterized EgGLUT1-ss as an important drug target against this larval stage and its inhibitor WZB117 as a candidate anti-CE drug.

Glucose metabolism pathway not only produces ATP for the physiological functions of eucaryote cells, but also provides an important source of carbon to support the biosynthesis of nucleotides and non-essential amino acids (29). *E. granulosus s.l.* produces ATP for its own growth by both aerobic and anaerobic carbohydrate metabolism pathways (30). Tsai *et al.* (12) and Zheng *et al.* (13) found that *E. granulosus s.l.* has complete glucose metabolism pathways, including glycolysis, the tricarboxylic acid cycle, and the pentose phosphate pathway. Wu *et al.* (31) showed that glycolytic enzyme, triosephosphate isomerase, as a drug target for the control of schistosomes (32) and of *Plasmodium* spp. (33), was also involved in the growth and development of *E. granulosus s.l.*. In addition, other glycolytic

232 enzymes, such as 6-phosphofructokinase 1 and pyruvate kinase, have been identified
233 in *E. granulosus s.l.* (34), and Hemer *et al.* (35) showed that the insulin receptor
234 pathway could regulate *E. multilocularis* glucose metabolism. In this study, we found
235 that suppressing the function of EgGLUT1-ss, a member of the glucose transporter 1
236 family that we cloned from *E. granulosus s.s.,* the species most frequently responsible
237 for CE worldwide, not only inhibited glucose uptake and ATP content by *E.*
238 *granulosus s.s.*, but also affected the viability of both vesicles and PSCs of *E.*
239 *granulosus s.s. in vitro* and cysts developed *in vivo*. Glucose, a polar and hydrophilic
240 molecule, cannot pass through hydrophobic cell membranes; GLUT1, which is
241 embedded in the cell membrane, carries out the function of glucose transport to
242 provide glucose supply (36-38). GLUT1-like transporters have been identified in
243 trypanosomes such as *T. brucei, and T. cruzi,* and in *Leishmania* spp. (39), as well as
244 in *E. multilocularis*, another species of the *Echinococcus* genus; in that species,
245 EmGLUT1 has a high glucose transport activity and likely plays an important role in
246 glucose uptake from its host at the larval stage (23). Like *E. multilocularis*, *E.*
247 *granulosus s.l.* is also dependent on its intermediate host-derived glucose; we may
248 thus suggest that EgGLUT1, a crucial upstream member of glucose metabolism
249 pathways acting as a switch for glucose to enter the parasite, serves as an
250 energy-provider from the host's glucose to the *E. granulosus s.l.* metacestode, and is
251 thus essential for its growth and survival.

252 The systemic anti-parasitic treatment of CE currently relies on the continuous

253 administration of either of two benzimidazole carbamates, ABZ and mebendazole,
254 which are the only drugs clinically efficient to interrupt the larval growth of *E.*
255 *granulosus s.l.* Both drugs interfere with glucose metabolism: their mechanism of
256 action has been associated with a marked inhibition of pyruvate kinase,
257 phosphoenolpyruvate carboxykinase and ATPase (40). In addition, a few bioenergetic
258 modulators have shown significant inhibition of parasite viability in preclinical *in vivo*
259 and *in vitro* experiments. As examples, 3-bromopyruvate which blocks glucose entry
260 into the glycolysis pathway by inhibiting hexokinase (HK) (41) has been shown to
261 inhibit *Echinococcus* spp. viability *in vitro* and *in vivo* (28); tacrolimus, a
262 rapamycin-target protein inhibitor, exerts anti-CE effects *in vivo* and *in vitro* and
263 affects the glucose metabolism of cysts *in vivo* (42); and metformin can reduce the
264 larval viability of *E. granulosus s.l.* by inhibiting its glucose metabolism pathway (43).
265 However, none of these compounds have succeeded in reaching the pre-clinical stage
266 of drug development for CE.

267 Synthetic GLUT1 inhibitors, such as BAY-876, WZB117 and STF-31, are still in
268 the pre-clinical research stage, but there are obvious experimental data showing that
269 the inhibition of glucose uptake they achieve has a real therapeutic potential (44-46).
270 Previous studies have reported that WZB117 significantly inhibits the proliferation of
271 cancer cells by reducing the transporter function of GLUT1 (47-49) which was
272 overexpressed in cancer cells (50), maybe through the reduction of ATP and glycolytic
273 enzyme levels. Resveratrol, which has a GLUT1 inhibitory effect, has been endorsed

by the FDA for the treatment of spinocerebellar ataxia (51). WZB117 was also shown to inhibit the growth of blood-stage *P. berghei* and reduce glucose uptake in the red blood cells by breaking redox balance (20). In our study, we found that GLUT1 inhibitor WZB117 significantly reduced the viability of *E. granulosus s.s.*. Our *in vitro* results showed that WZB117 inhibited the function of EgGLUT1-ss, leading to a reduction in glucose and ATP levels, which ultimately led to the death of both the PSCs and metacestode vesicles *in vitro*. In our *in vivo* experiments, we found that WZB117 achieved the same therapeutic results as ABZ, at a lower dose. The lower levels of glucose content in the cyst wall and the cyst fluid we found in the mice treated by WZB117 may suggest that WZB117 could be slightly more effective than ABZ; which may be due to the different targets of the two drugs, inhibition of cytoplasmic and mitochondrial malate dehydrogenase for ABZ (52) on one hand, and EgGLUT1-ss function in glucose uptake and transport for WZB117 on the other hand. The lower anti-CE effect of ABZ may also be related to its poor solubility, thus low cell availability, a well-known disadvantage for its clinical use in the treatment of echinococcosis (8-11). The dual and rapid effect of WZB117 on PSCs and the germinal layer of the metacestode is a supplementary advantage of the GLUT1 inhibitor for its use in CE in the peri-operative period to prevent the development of secondary cysts. Considering the rather frequent adverse effects of ABZ taken at the high dosage necessary to treat CE, and especially its liver toxicity often responsible for drug withdrawal in patients who depend on the drug for their survival (11),

295 WZB117 may likely become an alternative drug to ABZ not only for CE but also AE
296 for which ABZ use is inescapable.

297 Most of the candidate drugs that were promising, from *in vitro* and experimental
298 studies, against CE and AE have not reached the pre-clinical stage because of adverse
299 effects even superior to those of ABZ (53). Even though it is a promising strategy
300 for the treatment of CE, we cannot ignore the potential adverse effects of WZB117 on
301 the host. It has been previously reported that WZB117 inhibits facilitated glucose
302 transport by competing with sugars for occupancy of the exofacial substrate binding
303 site of the transporter (24). Prolonged inhibition of glucose transport could
304 compromise the normal cellular glycolysis of the host, affect host insulin secretion
305 and cause host's cerebral energy failure (54). Completing a thorough analysis of all
306 possible adverse events was beyond the scope of this study; however, we conducted a
307 preliminary safety assessment of WZB117 in its use to treat CE, in the murine
308 experimental model. We found no abnormalities in body weight and blood glucose in
309 our mice treated with WZB117 for 28 days. There were no significant changes in the
310 biological parameters under study, especially regarding liver toxicity. Our treatment
311 cycle was only 4 weeks; long-term safety still needs to be further evaluated, since
312 hyperglycemia and lipodystrophy were reported after long-term administration of
313 WZB117 (25); however, our data are very promising to launch pre-clinical studies on
314 peri-operative anti-parasitic treatment of CE, since 1 month is the usual recommended
315 duration of treatment in this situation. The results of our bioinformatics analysis show

316 that the GLUT1 gene sequences of *E. granulosus s.s.* differ significantly from other
317 species, which may true for all species within the *E. granulosus s.l.* cluster but this
318 should be specifically tested whenever the sequences of GLUT1 from other species
319 become available. The design of GLUT1 inhibitors more selective for the protein
320 structure of EgGLUT1 should also be the focus of future developments on CE drugs
321 to avoid interference with the host's GLUT1 while conserving therapeutic efficacy.

322 # Materials and methods

323 ## Chemicals

324 WZB117 and albendazole sulfoxide (ABZSO) were obtained from MedChem
325 Express (USA), and dimethyl sulfoxide (DMSO) and ABZ from Sigma (USA).

326 ## Ethics statement

327 All procedures carried out with animals were approved by the Ethical Committee
328 of the First Affiliated Hospital of Xinjiang Medical University
329 (IACUC-20130425012). At the end of treatment, all mice were euthanized to avoid
330 the pain of animals to the greatest extent.

331 ## Parasite collection and culture

332 Sterile PSCs were obtained aseptically from the cysts of sheep infected with *E.*
333 *granulosus sensu stricto* (*s.s.*) in the Hualing slaughter market of Urumqi in Xinjiang,
334 PR China. All experiments were conducted on this species. Viable and
335 morphologically intact PSCs were cultured using RPMI-1640 medium (Gibco, USA)
336 (10% fetal bovine serum, 100 U/ml penicillin, and 100 μg/ml streptomycin), and

337 maintained at 37°C under a humidified atmosphere containing 5% CO_2 (55, 56). For
338 *in vitro* experiments on *E. granulosus s.s.* metacestode, *in vitro* sterile cultures were
339 maintained for 4 months to obtain vesicles with a diameter of approximately 2 mm.

340 **Experimental infection of mice with *E. granulosus s.s.* PSCs**

341 Healthy female Kunming mice (20 ± 2 g of 8 weeks old) were adaptively reared
342 by the Experimental Animal Center of Xinjiang Medical University for one week
343 under controlled laboratory conditions (temperature 20 ± 2˚C and 50 ± 5% humidity)
344 (43). The mice were inoculated with 2,000 PSCs in 0.2 mL normal saline by
345 intraperitoneal injection. After 6 months, the mice were examined by B-scan
346 ultrasonography; when the diameter of the lesion was more than 0.5 cm, this indicated
347 that the infection was successful.

348 **WZB117 treatment *in vitro***

349 For a first set of experiments, after PSCs were cultured *in vitro* for one week,
350 their viability was tested by 1% eosin staining; to be used in the study, the required
351 percentage of viability required was higher than 90% (57). *In vitro* PSCs treatments
352 were performed with 3.125, 6.25, 12.5, 25, 50 and 100 μmol/L WZB117 (dissolved in
353 DMSO). For a second set of experiments, the PSC-derived vesicles were cultured *in*
354 *vitro* for four months and then cultured in a 6-well plate (25 vesicles /well). *In vitro*
355 vesicle treatments were performed with 3.125, 6.25, 12.5, 25, 50 and 100 μmol/L
356 WZB117 and 15 μmol/L ABZSO. For both control PSCs and vesicles, the culture
357 medium with an identical amount of DMSO (without inhibitor; final concentration,

1%) was used, and the PSCs and vesicles were cultured in an incubator (5% CO2, 37°C) for 4 days, and each viability test was repeated three times. The collapse of vesicles, loss of swelling and contraction of germinal layer were used as criteria for evaluating vesicle viability (58). Viability of PSCs and vesicles was observed under a microscope every 24 hours (59). Each experiment was performed in triplicate and repeated three times.

Glucose Uptake Assay

Glucose uptake levels were measured using the 2-[*N*-(7-nitrobenz-2-oxa-1,3-diazol-4-yl) amino]-2-deoxy-D-glucose (2-NBDG) (final concentration, 100 μmol/L) assay. Briefly, the PSCs with siRNA sequence or the WZB117-treated PSCs were incubated at 37℃ for 48 hours. Then, the PSCs were incubated in the darkness with 2-NBDG for 180 min and 60 min at 37°C in 5% CO_2 humidified atmosphere. The fluorescence intensity was detected at the excitation wavelength of 466 nm and emission wavelength of 540 nm by the fluorescence marker.

WZB117 treatment *in vivo*

For *in vivo* experiments, WZB117 was dissolved in PBS/DMSO (1:1, v/v) (25). All *E. granulosus s.s.*-infected mice (n = 45) judged appropriate at the 6th month after infection (see above) were randomly divided into five experimental groups: control group (receiving injections of the PBS/DMSO solvent), ABZ (50 mg/kg/day) group (60) and WZB117 (5, 10, 20 mg/kg/day) groups (20). After 28 days of continuous

379 intraperitoneal injection (dosage: 0.1 mL/10 g per mouse), animals were sacrificed by
380 cervical dislocation (57). At necropsy, the peritoneal cavity was opened, the number
381 of cysts was counted, cyst weights and diameters were measured. The efficacy of
382 treatments was calculated as follows: 100 × {(average cyst weight in the control
383 group) - (average cyst weight in the treatment group)} / (average cyst weight in the
384 control group) (57).

385 **Ultrastructure observations of WZB117 treated PSCs, vesicles, and cysts**

386 After *in vitro* and *in vivo* drug treatment, the PSCs, vesicles, or cysts were fixed
387 with 4% glutaraldehyde for 24 h (28). The samples were processed for SEM using a
388 JEOL1230 (JEOL company, Japan) microscope and TEM using a LEO1430VP (LEO
389 company, Germany) microscopy, as previously described.

390 **Glucose and ATP content measurements**

391 To determine the glucose and ATP content of cysts in treated mice, the cysts were
392 washed three times with precooled PBS and added with 100 μL of 20 mM Tris buffer
393 (Thermo, USA). The cyst wall was homogenized in a homogenizer for 2~4 minutes
394 and boiled in a water bath for 5 minutes before centrifugation (at 15,800 g at 4℃ for
395 30 min) (61). The cyst fluid was processed by gradient dilution according to the
396 instructions in the kit. Glucose Colorimetric Assay Kit (Cayman, USA) was used to
397 determine glucose contents. The ATP content was detected by the ATP Detection
398 Assay Kit (Cayman, USA). Each experiment was repeated three times.

399 **EgGLUT1-ss cloning**

Total RNA was extracted from *E. granulosus s.s.* PSCs by Mini BEST Universal RNA Extraction Kit (Takara, Japan). Me Script II 1st Strand cDNA Synthesis Kit (Takara, Japan) was reverse transcriptionally synthesized for 1st cDNA. The reaction conditions were: incubation at 42℃ for 60 min, heating at 95℃ for 5 min, termination of the reaction, and storage at -20℃ (62). We used the 1st cDNA synthesized by reverse transcription as a template and used the Premix Ex Taq™ Hot Start Version (Takara, Japan) to amplify the full-length sequence of the EgGLUT1-ss gene, primers for the target genes include: EgGLUT1-ss (forward primer 5'-ATGGTTAACTTTCACTACGT-3' and reverse primer 5'-CTAAAATCTGACCTTATCG-3'). The PCR amplification conditions were: pre-denaturation at 94℃ for 5 min; denaturation at 98℃ for 30 s; annealing at 45℃ for 30 s; extension at 72℃ for 90 s, for a total of 34 cycles. The reaction was terminated after 10 min extension at 72℃; 1% agarose gel was used to determine whether the gene band location was expected. PCR products of EgGLUT1-ss gene were recovered from Agarose Gel with Agarose Gel DNA Extraction Kit (Takara, Japan), and the amplified fragments were cloned into pMD19-T vector with Mighty ta-cloning Reagent Set for Prime STAR (Takara, Japan), and verified by sequencing. The gene was named as EgGLUT1-ss (accession number: MW393831).

Bioinformatics analysis and construction of the phylogenetic tree of GLUT1

The amino acid sequences of the homologous genes of GLUT1 in *E. multilocularis* (GenBank ID: CDS42031.1), *Hymenolepis microstoma* (GenBank ID:

421 CDS25463.1), *Caenorhabditis elegans* (GenBank ID: NP_493981.1), *Drosophila*
422 *melanogaster* (GenBank ID: NP_001097467.1), *Labrus bergylta* (GenBank ID:
423 XP_020502389.1), *Astyanax mexicanus* (GenBank ID: XP_007258287.2),
424 *Xiphophorus maculatus* (GenBank ID: XP_023187106.1), *Aplysia californica*
425 (GenBank ID: XP_012944940.1), *Biomphalaria glabrata* (GenBank ID:
426 XP_013087453.1), *Crassostrea gigas* (GenBank ID: XP_019925400.1), *Danio rerio*
427 (GenBank ID: NP_001034897.1), *Mus musculus* (GenBank ID: XP_006502971.1)
428 and *Homo sapiens* (GenBank ID: NP_006507.2) were obtained from GenBank. The
429 post-translational modification sites were predicted using the MotifScan software (63).
430 The transmembrane region was predicted using TMHMM (64). The conserved
431 domain was predicted using GenBank tools. The multiple sequence alignment was
432 analyzed by DNAMAN (Version 7.0.2.176). The phylogenetic tree was constructed
433 by MEGA (Version 10.0.5).

434 **EgGLUT1-ss-siRNA interference**

435 According to the cloned EgGLUT1-ss Gene sequence (accession number:
436 MW393831), siRNA interference sequences of three EgGLUT1-ss genes were
437 designed using Gene Pharma siRNA Designer 3.0 software. Experimental groups:
438 EgGLUT1-ss-treated groups (siRNA-386/578/723); negative control group (NC,
439 transfection independent interference sequence); untreated groups. The
440 siRNA-386/578/723 were transfected into PSCs cultured *in vitro* by electroporation.
441 The targeting sequence of each siRNA in EgGLUT1-ss cDNA is summarized in Table

1. The EgGLUT1-ss-siRNA interference assay was carried out as previously described (65). Briefly, Electroporation was performed at 125 V using a pulse. For electroporation, 200 μL electroporation buffer (5 mM magnesium chloride, 200 mM glucose, 20 mM Tris, 2 mM 2-Hydroxy-1-ethanethiol, pH adjusted to 7.4 with HCl) containing approximately 4,000 PSCs was placed in a 4-mm cuvette, and the final concentration of siRNA interference sequence was 5 μM. After electroporation, the shock cup was placed in a 37℃ incubator for 30 min and then transferred to a 6-well plate with 2 mL mixed medium for 48 h. After washing with PBS, PSCs in each group were stained with 1% eosin for 5 min, respectively. The viability was calculated on smears by counting using an inverted fluorescence microscope.

Quantitative real-time polymerase chain reaction (qRT-PCR) detection

Total RNA was extracted from PSCs and vesicles by Mini BEST Universal RNA Extraction Kit (Takara, Japan), as previously described (66). RNA was converted to cDNA with the PrimeScript™ RT reagent Kit Prime Script TMRT reagent Kit (Takara, Japan), and the cDNA was analyzed by qRT-PCR using TB Green® Premix Ex Taq™ II (Takara, Japan). The primer sequences are shown in Table 2. All samples were run in triplicate using the following cycle parameters: 95℃ for 30 s; 40 cycles at 95℃ for 5 s and 55℃ for 30 s; 72℃ for 1 min; from 95℃, the temperature dropped to 65℃ at a rate of 20.0℃/s. After incubation for 15 s at 65℃, the temperature was increased to 95℃ at a rate of 20.0℃/s. All data were used for standard curve analysis.

Docking study

463 Through the Pubchem website (https://pubchem.ncbi.nlm.nih.gov/) to retrieve
464 the 3D structure of WZB117, we adopted the Autodock software (version 4.2.6) to
465 hydrogenation processing, calculating charge EgGLUT1-ss protein, and setting the
466 receptor proteins docking lattice parameter. We used AutoDock Vina (version 1.1.2) to
467 dock EgGLUT1-ss and WZB117 and obtained 20 conformations. EgGLUT1-ss and
468 WZB117 were used to chart the binding sites and amino acid residues and PyMOL
469 (version 2.4.0) was used as a 3D diagram to show the interaction between receptor
470 proteins and ligand small molecules.

471 **Statistical analysis**

472 For the comparison between experimental and control data, Student's t-test and
473 chi-square test were used to determine its significance. All data were expressed as
474 (arithmetic mean ± standard deviation), and *P* values are indicated in each assay (**P* <
475 0.05, ***P* < 0.01). All analyses were performed using IBM SPSS Statistics 20
476 software.

477 **Linguistic statement**

478 The terminology proposed by the World Association of Echinococcosis was
479 followed all along the text of the publication. Especially, we followed the distinction
480 between 'vesicles', obtained *in vitro*, and 'cysts' obtained from *in vivo* experiments,
481 and between *E. granulosus sensu lato* for the cluster of species previously known as
482 '*E. granulosus'* and '*E. granulosus sensu stricto'* for the species used in our
483 experiments (67).

Acknowledgements

This research was supported by the National Natural Science Foundation of China (NSFC) (82060373, 81760369 and 81360251); State Key Laboratory of Pathogenesis, Prevention and Treatment of Central Asian High Incidence Diseases Fund (SKL-HIDCA-2020-BC3); "Tianshan Cedar" Science and Technology Innovation Talents Support Plan of Xinjiang Uygur Autonomous Region (No. 2019XS13). The funders had no role in study design, data collection and interpretation, or the decision to submit the work for publication.

We thank Zhiqiang Li of the Animal Experiment Center of Xinjiang Medical University for providing help with animal experiments and Haiyan Ren of the Department of Electron Microscopy of Xinjiang Medical University for providing technical support in the use of electron microscopes.

Transparency declarations

None to declare.

References

1. Larrieu E, Gavidia CM, Lightowlers MW. 2019. Control of cystic echinococcosis: Background and prospects. Zoonoses Public Health 66:889-899.

2. Wen H, Vuitton L, Tuxun T, Li J, Vuitton DA, Zhang W, McManus DP. 2019. Echinococcosis: Advances in the 21st Century. Clin Microbiol Rev 32: e00075-18.

3. Agudelo Higuita NI, Brunetti E, McCloskey C. 2016. Cystic Echinococcosis. J Clin Microbiol 54:518-23.

4. Craig PS, McManus DP, Lightowlers MW, Chabalgoity JA, Garcia HH, Gavidia CM, Gilman RH, Gonzalez AE, Lorca M, Naquira C, Nieto A, Schantz PM. 2007. Prevention and control of cystic echinococcosis. Lancet Infect Dis 7:385-94.

5. WHO. 2019 [cited 1 Nov 2019]. Echinococcosis. https://www.who.int/news-room/fact-sheets/detail/echinococcosis.

6. Budke CM, Deplazes P, Torgerson PR. 2006. Global socioeconomic impact of cystic echinococcosis. Emerg Infect Dis 12:296-303.

7. Qian MB, Zhou XN. 2018. Walk together to combat echinococcosis. Lancet Infect Dis 18:946.

8. Brunetti E, Kern P, Vuitton DA. 2010. Expert consensus for the diagnosis and treatment of cystic and alveolar echinococcosis in humans. Acta Trop 114:1-16.

9. Kern P, Menezes da Silva A, Akhan O, Müllhaupt B, Vizcaychipi KA, Budke C, Vuitton DA. 2017. The Echinococcoses: Diagnosis, Clinical Management and Burden of Disease. Adv Parasitol 96:259-369.

10. Horton J. 2002. Albendazole: a broad spectrum anthelminthic for treatment of individuals and populations. Curr Opin Infect Dis 15:599-608.

11. Horton J. 2003. Albendazole for the treatment of echinococcosis. Fundam Clin Pharmacol 17:205-12.

12. Tsai IJ, Zarowiecki M, Holroyd N, Garciarrubio A, Sanchez-Flores A, Brooks KL, Tracey A, Bobes RJ, Fragoso G, Sciutto E, Aslett M, Beasley H, Bennett HM, Cai X, Camicia F, Clark R, Cucher M, De Silva N, Day TA, Deplazes P, Estrada K, Fernandez C, Holland PWH, Hou J, Hu S, Huckvale T, Hung SS, Kamenetzky L, Keane JA, Kiss F, Koziol U, Lambert O, Liu K, Luo X, Luo Y, Macchiaroli N, Nichol S, Paps J, Parkinson J, Pouchkina-Stantcheva N, Riddiford N, Rosenzvit M, Salinas G, Wasmuth JD, Zamanian M, Zheng Y, Cai J, Soberon X, Olson PD, Laclette JP, et al. 2013. The genomes of four tapeworm species reveal adaptations to parasitism. Nature 496:57-63.

13. Zheng H, Zhang W, Zhang L, Zhang Z, Li J, Lu G, Zhu Y, Wang Y, Huang Y, Liu J, Kang H, Chen J, Wang L, Chen A, Yu S, Gao Z, Jin L, Gu W, Wang Z, Zhao L, Shi B, Wen H, Lin R, Jones MK, Brejova B, Vinar T, Zhao G, McManus DP, Chen Z, Zhou Y, Wang S. 2013. The genome of the hydatid tapeworm Echinococcus granulosus. Nat Genet 45:1168-75.

14. Wang Y, He T, Wen X, Li T, Waili A, Zhang W, Xu X, Vuitton DA, Rogan MT, Wen H, Craig PS. 2006. Post-survey follow-up for human cystic echinococcosis in northwest China. Acta Trop 98:43-51.

15. Son DS, Lee ES, Adunyah SE. 2020. The Antitumor Potentials of Benzimidazole Anthelmintics as Repurposing Drugs. Immune Netw 20:e29.

16. Takata K, Kasahara T, Kasahara M, Ezaki O, Hirano H. 1990. Erythrocyte/HepG2-type glucose transporter is concentrated in cells of blood-tissue barriers. Biochem Biophys Res Commun 173:67-73.

17. Xiao H, Wang J, Yan W, Cui Y, Chen Z, Gao X, Wen X, Chen J. 2018. GLUT1 regulates cell glycolysis and proliferation in prostate cancer. Prostate 78:86-94.

18. Li YL, Weng HC, Hsu JL, Lin SW, Guh JH, Hsu LC. 2019. The Combination of MK-2206 and WZB117 Exerts a Synergistic Cytotoxic Effect Against Breast Cancer Cells. Front Pharmacol 10:1311.

19. Bertrand L, Auquier J, Renguet E, Angé M, Cumps J, Horman S, Beauloye C. 2020. Glucose transporters in cardiovascular system in health and disease. Pflugers Arch 472:1385-1399.

20. Wei M, Lu L, Sui W, Liu Y, Shi X, Lv L. 2018. Inhibition of GLUTs by WZB117 mediates apoptosis in blood-stage Plasmodium parasites by breaking redox balance. Biochem Biophys Res Commun 503:1154-1159.

21. Michels PA, Bringaud F, Herman M, Hannaert V. 2006. Metabolic functions of glycosomes in trypanosomatids. Biochim Biophys Acta 1763:1463-77.

22. Borst P, Fairlamb AH. 1998. Surface receptors and transporters of Trypanosoma brucei. Annu Rev Microbiol 52:745-78.

565 23. Kashiide T, Kikuta S, Yamaguchi M, Irie T, Kouguchi H, Yagi K, Matsumoto
566 J. 2018. Molecular and functional characterization of glucose transporter
567 genes of the fox tapeworm Echinococcus multilocularis. Mol Biochem
568 Parasitol 225:7-14.
569 24. Ojelabi OA, Lloyd KP, Simon AH, De Zutter JK, Carruthers A. 2016.
570 WZB117 (2-Fluoro-6-(m-hydroxybenzoyloxy) Phenyl m-Hydroxybenzoate)
571 Inhibits GLUT1-mediated Sugar Transport by Binding Reversibly at the
572 Exofacial Sugar Binding Site. J Biol Chem 291:26762-26772.
573 25. Liu Y, Cao Y, Zhang W, Bergmeier S, Qian Y, Akbar H, Colvin R, Ding J,
574 Tong L, Wu S, Hines J, Chen X. 2012. A small-molecule inhibitor of glucose
575 transporter 1 downregulates glycolysis, induces cell-cycle arrest, and inhibits
576 cancer cell growth in vitro and in vivo. Mol Cancer Ther 11:1672-82.
577 26. Hruz PW, Mueckler MM. 2001. Structural analysis of the GLUT1 facilitative
578 glucose transporter (review). Mol Membr Biol 18:183-93.
579 27. Vinaud MC, Ambrosio J. 2020. Metabolic effects of anthelminthic drugs in
580 the larval stage of the cestode Taenia crassiceps, cysticercosis experimental
581 model - A review. Acta Trop 206:105448.
582 28. Xin Q, Yuan M, Li H, Song X, Lu J, Jing T. 2019. In vitro and in vivo effects
583 of 3-bromopyruvate against Echinococcus metacestodes. Vet Res 50:96.
584 29. Zhu J, Thompson CB. 2019. Metabolic regulation of cell growth and
585 proliferation. Nat Rev Mol Cell Biol 20:436-450.

30. Cui SJ, Xu LL, Zhang T, Xu M, Yao J, Fang CY, Feng Z, Yang PY, Hu W, Liu F. 2013. Proteomic characterization of larval and adult developmental stages in Echinococcus granulosus reveals novel insight into host-parasite interactions. J Proteomics 84:158-75.

31. Wu M, Yan M, Xu J, Yin X, Dong X, Wang N, Gu X, Xie Y, Lai W, Jing B, Peng X, Yang G. 2018. Molecular characterization of triosephosphate isomerase from Echinococcus granulosus. Parasitol Res 117:3169-3176.

32. Chen B, Wen JF. 2011. The adaptive evolution divergence of triosephosphate isomerases between parasitic and free-living flatworms and the discovery of a potential universal target against flatworm parasites. Parasitol Res 109:283-9.

33. Velanker SS, Ray SS, Gokhale RS, Suma S, Balaram H, Balaram P, Murthy MR. 1997. Triosephosphate isomerase from Plasmodium falciparum: the crystal structure provides insights into antimalarial drug design. Structure 5:751-61.

34. Pan W, Shen Y, Han X, Wang Y, Liu H, Jiang Y, Zhang Y, Wang Y, Xu Y, Cao J. 2014. Transcriptome profiles of the protoscoleces of Echinococcus granulosus reveal that excretory-secretory products are essential to metabolic adaptation. PLoS Negl Trop Dis 8:e3392.

35. Hemer S, Konrad C, Spiliotis M, Koziol U, Schaack D, Förster S, Gelmedin V, Stadelmann B, Dandekar T, Hemphill A, Brehm K. 2014. Host insulin

606 stimulates Echinococcus multilocularis insulin signalling pathways and larval
607 development. BMC Biol 12:5.
608 36. Baldwin SA, Barros LF, Griffiths M. 1995. Trafficking of glucose
609 transporters--signals and mechanisms. Biosci Rep 15:419-26.
610 37. Macheda ML, Rogers S, Best JD. 2005. Molecular and cellular regulation of
611 glucose transporter (GLUT) proteins in cancer. J Cell Physiol 202:654-62.
612 38. Tetaud E, Barrett MP, Bringaud F, Baltz T. 1997. Kinetoplastid glucose
613 transporters. Biochem J 325 (Pt 3):569-80.
614 39. Rodriguez-Contreras D, Landfear SM. 2014. Transporters, channels and
615 receptors in flagella. Channels (Austin) 8:477-8.
616 40. Hernández-Luis F, Hernández-Campos A, Castillo R, Navarrete-Vázquez G,
617 Soria-Arteche O, Hernández-Hernández M, Yépez-Mulia L. 2010. Synthesis
618 and biological activity of 2-(trifluoromethyl)-1H-benzimidazole derivatives
619 against some protozoa and Trichinella spiralis. Eur J Med Chem 45:3135-41.
620 41. Ko YH, Pedersen PL, Geschwind JF. 2001. Glucose catabolism in the rabbit
621 VX2 tumor model for liver cancer: characterization and targeting hexokinase.
622 Cancer Lett 173:83-91.
623 42. Muhedier M, Li J, Liu H, Ma G, Amahong K, Lin R, Lü G. 2020. Tacrolimus,
624 a rapamycin target protein inhibitor, exerts anti-cystic echinococcosis effects
625 both in vitro and in vivo. Acta Trop 212:105708.

626 43. Loos JA, Cumino AC. 2015. In Vitro Anti-Echinococcal and Metabolic
627 Effects of Metformin Involve Activation of AMP-Activated Protein Kinase in
628 Larval Stages of Echinococcus granulosus. PLoS One 10:e0126009.
629 44. Ma Y, Wang W, Idowu MO, Oh U, Wang XY, Temkin SM, Fang X. 2018.
630 Ovarian Cancer Relies on Glucose Transporter 1 to Fuel Glycolysis and
631 Growth: Anti-Tumor Activity of BAY-876. Cancers (Basel) 11.
632 45. Peng Y, Xing SN, Tang HY, Wang CD, Yi FP, Liu GL, Wu XM. 2019.
633 Influence of glucose transporter 1 activity inhibition on neuroblastoma in vitro.
634 Gene 689:11-17.
635 46. Matsumoto T, Jimi S, Migita K, Takamatsu Y, Hara S. 2016. Inhibition of
636 glucose transporter 1 induces apoptosis and sensitizes multiple myeloma cells
637 to conventional chemotherapeutic agents. Leuk Res 41:103-10.
638 47. Chen Q, Meng YQ, Xu XF, Gu J. 2017. Blockade of GLUT1 by WZB117
639 resensitizes breast cancer cells to adriamycin. Anticancer Drugs 28:880-887.
640 48. Koch A, Lang SA, Wild PJ, Gantner S, Mahli A, Spanier G, Berneburg M,
641 Müller M, Bosserhoff AK, Hellerbrand C. 2015. Glucose transporter isoform 1
642 expression enhances metastasis of malignant melanoma cells. Oncotarget
643 6:32748-60.
644 49. Vander Heiden MG, Cantley LC, Thompson CB. 2009. Understanding the
645 Warburg effect: the metabolic requirements of cell proliferation. Science
646 324:1029-33.

647 50. Ganapathy V, Thangaraju M, Prasad PD. 2009. Nutrient transporters in cancer:
648 relevance to Warburg hypothesis and beyond. Pharmacol Ther 121:29-40.
649 51. Meng Y, Xu X, Luan H, Li L, Dai W, Li Z, Bian J. 2019. The progress and
650 development of GLUT1 inhibitors targeting cancer energy metabolism. Future
651 Med Chem 11:2333-2352.
652 52. Tejada P, Sanchez-Moreno M, Monteoliva M, Gomez-Banqueri H. 1987.
653 Inhibition of malate dehydrogenase enzymes by benzimidazole anthelmintics.
654 Vet Parasitol 24:269-74.
655 53. Schein CH. 2020. Repurposing approved drugs on the pathway to novel
656 therapies. Med Res Rev 40:586-605.
657 54. Brockmann K. 2009. The expanding phenotype of GLUT1-deficiency
658 syndrome. Brain Dev 31:545-52.
659 55. Wang H, Li J, Zhang C, Guo B, Wei Q, Li L, Yang N, Peter McManus D, Gao
660 X, Zhang W, Wen H. 2018. Echinococcus granulosus sensu stricto: silencing
661 of thioredoxin peroxidase impairs the differentiation of protoscoleces into
662 metacestodes. Parasite 25:57.
663 56. Walker M, Rossignol JF, Torgerson P, Hemphill A. 2004. In vitro effects of
664 nitazoxanide on Echinococcus granulosus protoscoleces and metacestodes. J
665 Antimicrob Chemother 54:609-16.
666 57. Loos JA, Davila VA, Rodrigues CR, Petrigh R, Zoppi JA, Crocenzi FA,
667 Cumino AC. 2017. Metformin exhibits preventive and therapeutic efficacy

668 against experimental cystic echinococcosis. PLoS Negl Trop Dis
669 11:e0005370.
670 58. Elissondo M, Ceballos L, Dopchiz M, Andresiuk V, Alvarez L, Bruni SS,
671 Lanusse C, Denegri G. 2007. In vitro and in vivo effects of flubendazole on
672 Echinococcus granulosus metacestodes. Parasitol Res 100:1003-9.
673 59. Fabbri J, Maggiore MA, Pensel PE, Denegri GM, Gende LB, Elissondo MC.
674 2016. In vitro and in vivo efficacy of carvacrol against Echinococcus
675 granulosus. Acta Trop 164:272-279.
676 60. Wen H, New RR, Muhmut M, Wang JH, Wang YH, Zhang JH, Shao YM,
677 Craig PS. 1996. Pharmacology and efficacy of liposome-entrapped
678 albendazole in experimental secondary alveolar echinococcosis and effect of
679 co-administration with cimetidine. Parasitology 113 (Pt 2):111-21.
680 61. You H, Zhang W, Moertel L, McManus DP, Gobert GN. 2009.
681 Transcriptional profiles of adult male and female Schistosoma japonicum in
682 response to insulin reveal increased expression of genes involved in growth
683 and development. Int J Parasitol 39:1551-9.
684 62. Cumino AC, Lamenza P, Denegri GM. 2010. Identification of functional FKB
685 protein in Echinococcus granulosus: its involvement in the protoscolicidal
686 action of rapamycin derivates and in calcium homeostasis. Int J Parasitol
687 40:651-61.

688 63. Rai S, Agrawal C, Shrivastava AK, Singh PK, Rai LC. 2014. Comparative
689 proteomics unveils cross species variations in Anabaena under salt stress. J
690 Proteomics 98:254-70.
691 64. Gulyaeva AA, Sigorskih AI, Ocheredko ES, Samborskiy DV, Gorbalenya AE.
692 2020. LAMPA, LArge Multidomain Protein Annotator, and its application to
693 RNA virus polyproteins. Bioinformatics 36:2731-2739.
694 65. Mizukami C, Spiliotis M, Gottstein B, Yagi K, Katakura K, Oku Y. 2010.
695 Gene silencing in Echinococcus multilocularis protoscoleces using RNA
696 interference. Parasitol Int 59:647-52.
697 66. Li J, Zhang WB, McManus DP. 2004. Recombinant antigens for
698 immunodiagnosis of cystic echinococcosis. Biol Proced Online 6:67-77.
699 67. Vuitton DA, McManus DP, Rogan MT, Romig T, Gottstein B, Naidich A,
700 Tuxun T, Wen H, Menezes da Silva A. 2020. International consensus on
701 terminology to be used in the field of echinococcoses. Parasite 27:41.
702

Figures

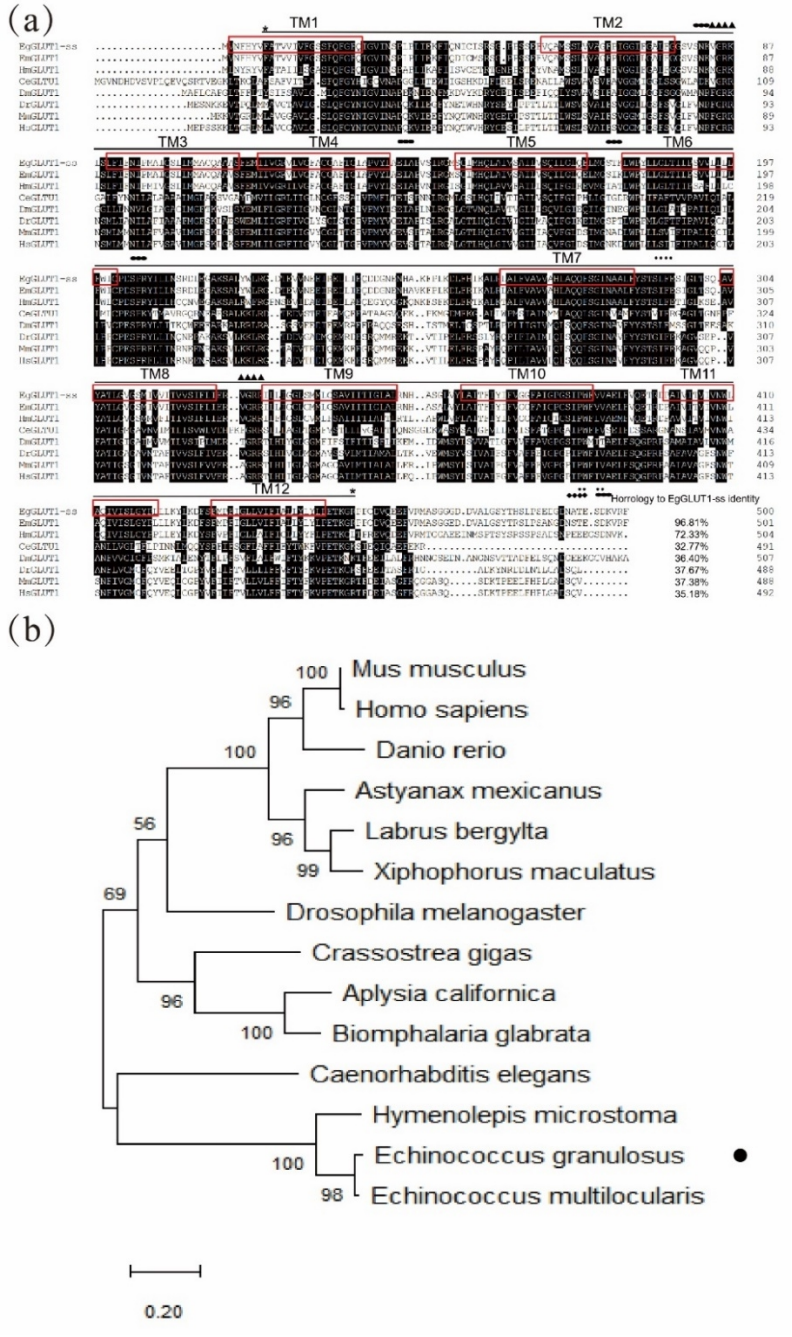

Figure 1. EgGLUT1-ss bioinformatics analysis and its expression level in the metacestode of *E. granulosus s.s.* (a) Multiple-sequence alignments of EgGLUT1-ss from *E. granulosus s.s.* (accession number: MW393831); *Echinococcus multilocularis* (accession number CDS42031.1); *Hymenolepis microstoma* (accession

709 number CDS25463.1); *Caenorhabditis elegans* (accession number NP_493981.1);
710 *Drosophila melanogaster* (accession number NP_001097467.1); *Danio rerio*
711 (accession number NP_001034897.1); *Mus musculus* (accession number
712 XP_006502971.1); and *Homo sapiens* (accession number NP_006507.2). The
713 horizontal line between the two * represents the MFS super family; (▲) denotes the
714 amidation site; (◆) denotes the glycosylation site; (·) denotes Casein kinase II
715 phosphorylation site; (⬬) denotes protein kinase C phosphorylation site; The red box
716 represents the transmembrane (TM) region. (b) Phylogenetic tree constructed using
717 the neighbor-joining method to compare the relationship between EgGLUT1-ss and
718 GLUT1 from other species. The numbers above the branches refer to bootstrap values.
719 The species for sequences included in the phylogenetic analysis are shown behind the
720 branches. EgGLUT1-ss from *E. granulosus s.s.* is indicated by •.
721

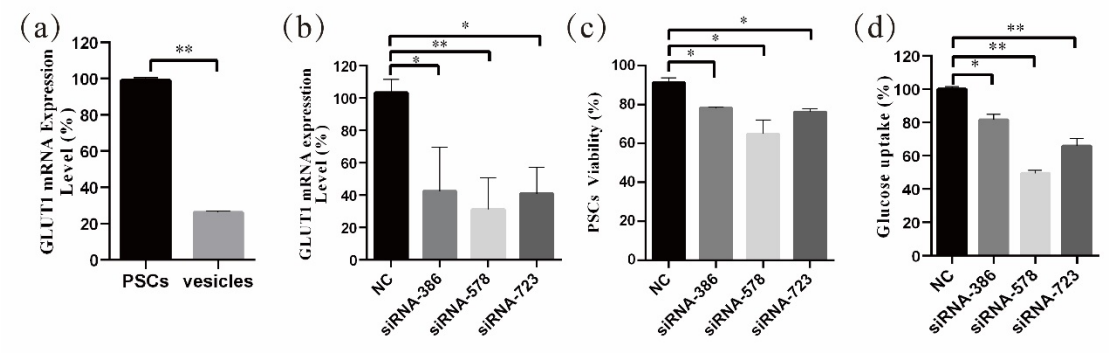

Figure 2. EgGLUT1-ss Knockdown reduces the viability and glucose uptake of PSCs. (a) EgGLUT1-ss mRNA expression in PSCs and vesicles. (b) EgGLUT1-ss mRNA expression at 48 h after siRNA-386/578/723 interference. (c) PSCs viability at 48 h after siRNA-386/578/723 interference. (d) Glucose uptake of PSCs at 48 h after siRNA-386/578/723 interference. NC: negative control group (transfection by independent interference sequence). * and ** indicate that the difference was statistically significant (*$P < 0.05$; **$P < 0.01$).

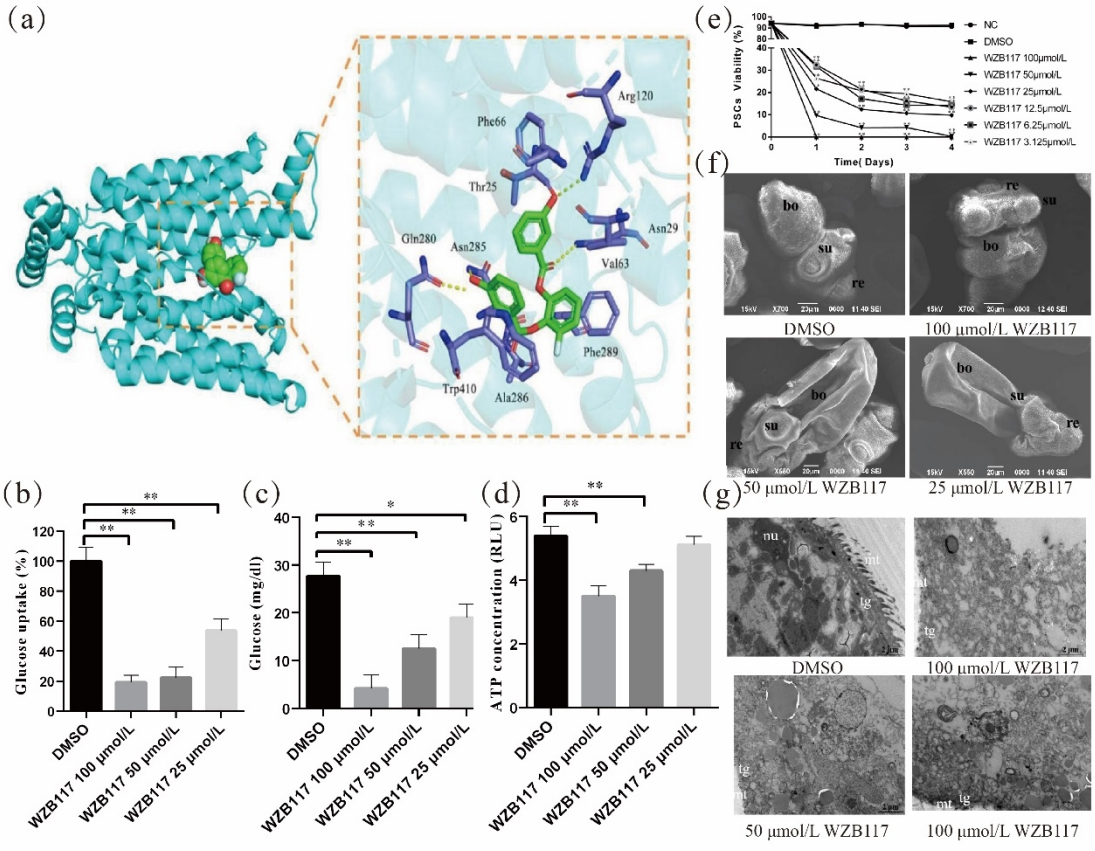

730

731 **Figure 3. WZB117 inhibits glucose metabolism and reduces the viability of PSCs**

732 ***in vitro*.** (a) Docked structure and interactions of WZB117 binding to EgGLUT1-ss.

733 The image on the left shows that WZB11 binds to the central channel region of

734 EgGLUT1-ss. The image on the right shows the detailed interactions (formation of 4

735 hydrogen bonds) between WZB117 and amino acid residues of EgGLUT1-ss. (b)

736 Glucose uptake of PSCs after WZB117 incubation for 60 min. (c) Glucose content of

737 PSCs after WZB117 incubation for 48 h. (d) ATP content of PSCs after WZB117

738 incubation for 48 h. (e) PSCs viability after WZB117 intervention for 4 days. Data are

739 the mean ± S.D. of three independent experiments. (f) Representative SEM images of

740 PSCs after WZB117 incubation for 4 days. PSCs incubated in culture medium

741 containing DMSO served as a control. (g) Representative TEM images of PSCs after

742 WZB117 intervention for 4 days. PSCs incubated in culture medium containing
743 DMSO served as a control. NC: negative control group; DMSO: control group. * and
744 ** indicate that the difference was statistically significant (*$P < 0.05$, **$P < 0.01$)
745 compared with control group. re, rostellum; su, suckers; bo, body; mt, microtriches;
746 nu, nucleus; tg, tegument.

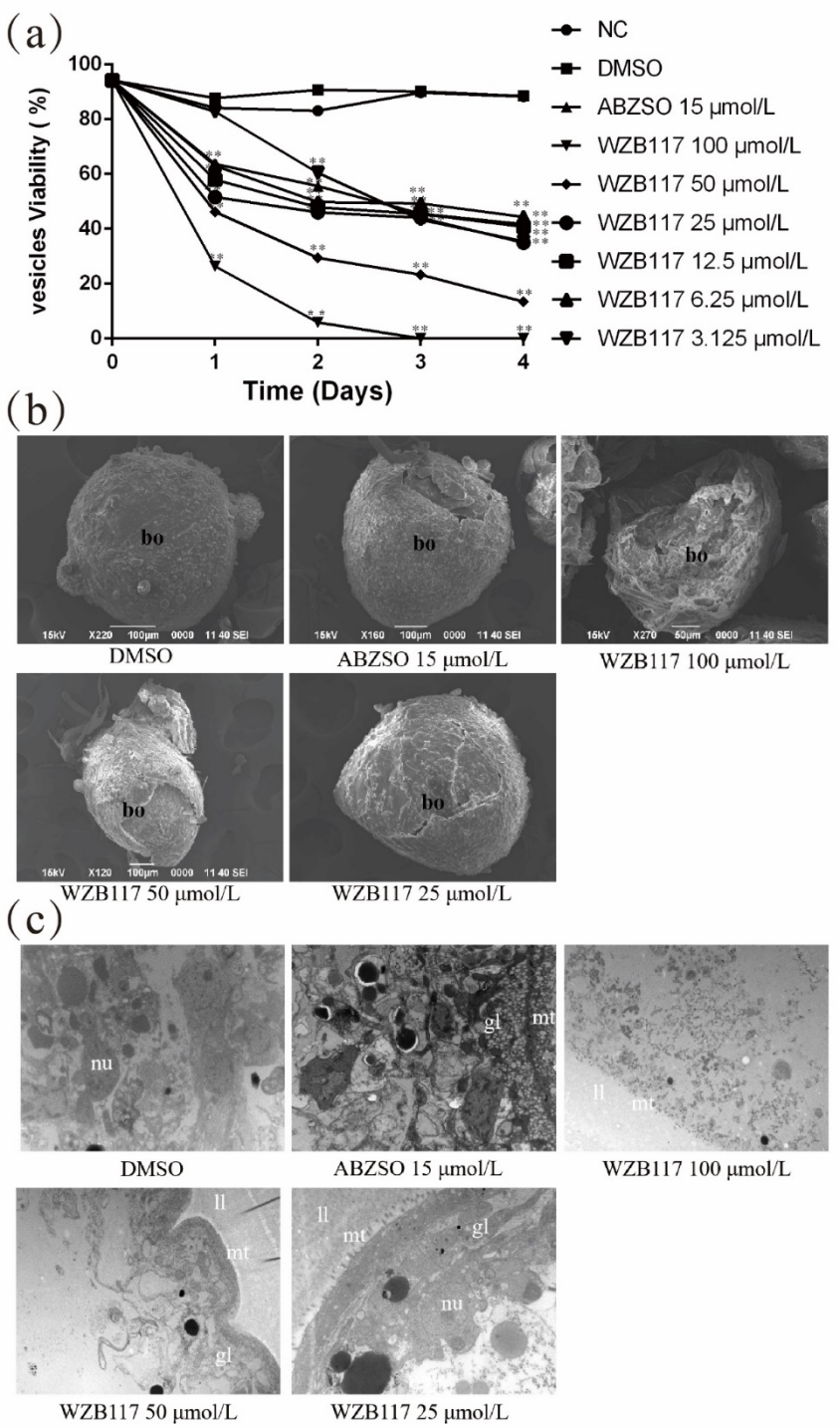

747

748 **Figure 4. WZB117 reduces the viability of *E. granulosus s.s.* vesicles *in vitro*.** (a)

749 Vesicle viability of *E. granulosus s.s.* after WZB117 incubation for 4 days. NC:

750 negative control group; DMSO: control group. * and ** indicate that the difference

751 was statistically significant (*$P < 0.05$, **$P < 0.01$) compared with control group. (b)

752 Representative SEM images of vesicles after WZB117 incubation for 4 days. Vesicles
753 incubated in culture medium containing DMSO served as a control. (c) Representative
754 TEM images of vesicles after WZB117 incubation for 4 days. Vesicles incubated in
755 culture medium containing DMSO served as a control. bo, body; gl, germinal layer; ll,
756 laminated layer; mt, microtriches; nu, nucleus.

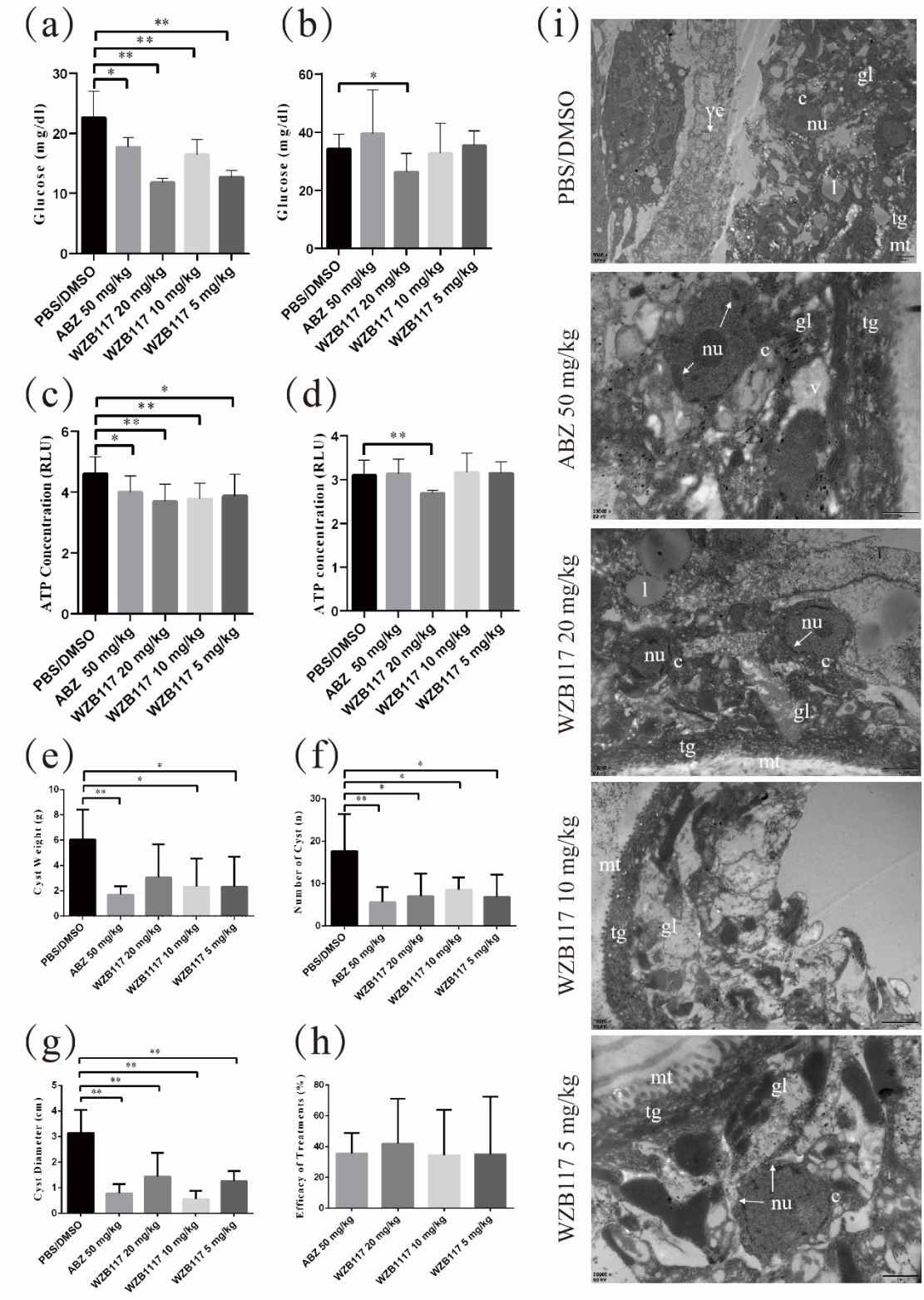

Figure 5. WZB117 treatment effectively inhibits the growth of cysts and reduces glucose and ATP levels in *E. granulosus s.s.*-infected mice. (a) Glucose content of

760 cyst tissue in *E. granulosus s.s.*-infected mice after WZB117 treatment for 28 days. (b)
761 Glucose content in the cyst fluid after WZB117 treatment for 28 days. (c) ATP
762 content in the cyst tissue. (d) ATP content in the cyst fluid. (e) Cyst weight in *E.*
763 *granulosus s.s.*-infected mice. (f) Cyst number in *E. granulosus s.s.*-infected mice. (g)
764 Cyst diameter in *E. granulosus s.s.*-infected mice. (h) Efficacy of 28-days treatments
765 in *E. granulosus s.s.*-infected mice. (i) Representative TEM images of cysts in *E.*
766 *granulosus s.s.*-infected mice. PBS/DMSO: control group. * and ** indicate that the
767 difference was statistically significant (*$P < 0.05$, **$P < 0.01$) compared with control
768 group. gl, germinal layer; ll, laminated layer; tg, tegument; l, lipid droplet; mt,
769 microtriches; nu, nucleus; c, cell; arrow, broken nucleus.

770 **Table 1. Design of the potential three siRNA sequences targeting EgGLUT1-ss**

771 **gene**

siRNA ID	Sense sequences	Antisense sequences
siRNA-386	GGAUUGAACCUGGUCCGAUTT	AUCGGACCAGGUUCAAUCCTT
siRNA-578	CCACGGUGAUGACAACAAUTT	AUUGUUGUCAUCACCGUGGTT
siRNA-723	GGCAACAAAGAGAGCCAAATT	UUUGGCUCUCUUUGUUGCCTT

772

773

774 **Table 2. EgGLUT1-ss Gene primer sequences**

Gene	Primer	Sequence 5'-3'
EgGLUT1-ss	Fw	5′- TTCTTCTTATAGGCGGTCTC -3′
	Rv	5′- AGGTGATGGCAAGGTAGA -3′
β-actin	Fw	5′-GCGATGTATGTAGCTATCCAGGCAGTGCTCTCGCT-3′
	Rv	5′-CAATCCAGACAGAGTATTTGCGTTCCGGAGGA-3′

775